



Energetics of graphene origami and their “spatial resolution”

Yang Yang, Zhuhua Zhang, Zhili Hu, Evgeni S. Penev, and Boris I. Yakobson*

Submitted September 8, 2020; Accepted November 17, 2020 ; published online: 18 January 2021

The flexibility and foldability of graphene are some of its attractive properties inspiring the designs of origami structures with potential use in flexible electronics and electromechanical nanodevices. The aesthetics, precision, and ease of folding and stability, however, have limitations at the nanoscale. Here, by means of large-scale atomistic calculations and continuum models, it is quantified how the dimensions determine the relative robustness of the elementary folds of graphene (a single fold and a double-folded graphene forming a single order-four vertex), thereby mapping the spatial resolution limits and providing important guidance for graphene nano-origami realizations.

The extreme thinness of graphene combined with its tensile strength made it a material appealing for discussing and even making complex cut-kirigami or folded-only origami. In the case of origami, its stability is mainly defined by the positive energy of the single- or double-fold curvature deformation counterbalanced by the energy reduction due to favorable van der Waals contacts. These opposite sign contributions also have notably different scaling with the size L of the construction, the contacts contributing in proportion to area $\sim L^2$, single folds as $\sim L$, and highly strained double-fold corners as only $\sim L^0 = \text{const}$. Computational analysis with realistic atomistic-elastic representation of graphene allows one to quantify these energy contributions and to establish the length scale, where a single fold is favored ($7 \text{ nm} < L < 21 \text{ nm}$) or a double fold becomes sustainable ($L > 21 \text{ nm}$), defining the size of the smallest possible complex origami designs as $L \gg 21 \text{ nm}$.

Introduction

Graphene, a two-dimensional monolayer in the form of a honeycomb lattice, has sparked an avalanche of research activities due to a series of outstanding properties and potential applications. It is considered among the strongest materials ever reported, with an in-plane stiffness $C = 345 \text{ N/m}$ equivalent to 1 TPa ^{1,2} and tensile strength of more than 100 GPa .^{3–6} On the other hand, graphene is flexible against out-of-plane deformation because of its low bending stiffness of $\sim 1.5 \text{ eV}$.^{1,7,8} The unique combination of the extremely high in-plane stiffness with small out-of-plane bending modulus suggests graphene as a unique building material component for fabricating origami

mechanologic in flexible electronics⁹ as well as in nanoelectromechanical devices.¹⁰

Recently, an experimental work shows that graphene can act as a paper, suitable for folding nontrivial origami structures, which allows the use of graphene to build 3D microscopic structures with tunable mechanical properties and designed functionalities.¹¹ In the produced origami structures, graphene unavoidably undergoes various deformations, such as stretching and bending. In particular, the bending deformations have a rich variety of forms and are crucial to the stability of graphene origami, a pre-designed or arbitrarily crumpled 3D object made of planar 2D sheet-material, confined within a volume $\sim L^3$. First,

Yang Yang, Department of Materials Science and NanoEngineering, Rice University, Houston, TX, USA
 Zhuhua Zhang, State Key Laboratory of Mechanics and Control of Mechanical Structures, Key Laboratory for Intelligent Nano Materials and Devices of Ministry of Education, Institute of Nano Science, Nanjing University of Aeronautics and Astronautics, Nanjing, China
 Zhili Hu, State Key Laboratory of Mechanics and Control of Mechanical Structures, Key Laboratory for Intelligent Nano Materials and Devices of Ministry of Education, Institute of Nano Science, Nanjing University of Aeronautics and Astronautics, Nanjing, China
 Evgeni S. Penev, Department of Materials Science and NanoEngineering, Rice University, Houston, TX, USA
 Boris I. Yakobson, Department of Materials Science and NanoEngineering, Rice University, Houston, TX, USA; biy@rice.edu
 *Corresponding author.
 doi:10.1557/s43577-020-00018-8



folding graphene inevitably needs to overcome the bending energy concentrated in the folds-ridges (bilayer edges¹²) of length scale $\sim L$. The stabilization of such folded graphene is by energy gain from van der Waals (vdW) attraction in the contact-stacking regions, scaling as $\sim -L^2$. Since the vdW energy is proportional to the folded area, there should exist a critical size of graphene above which the energy change ($\text{const} \times L - \text{const}' \times L^2$) turns negative, and folded structures can be thermodynamically favorable or at least metastable. To the best of our knowledge, the question of what this critical size is remains unanswered. Second, the construction of more complicated origami structures often requires more than single folding of graphene. A double fold involves much more mechanical distortion when formed, and there will be an additional energy cost for the four-layer folding corner, or vertex (circle in **Figure 1b**), which is positive and tends to destabilize the double-folded structure. Although the contribution of such corners scales as only $\sim L^0$, their energy is quite high and cannot be overlooked. Similarly, it contributes in a generic origami structure such as origami waterbomb, whose bistability is central for mechanologic.⁹ Evaluating the smallest length scale from graphene’s physical properties should in turn define the memory or other origami-associated functionality spatial density, or “spatial resolution” $\sim L$ of the smallest features in any complex origami sustained mechanically.

A question arises as to how to quantify the contributions of different scaling with the size L , and, in particular, what is the energy cost of the double-fold corners/vertices? To shed light on this problem, it is necessary to perform extensive computations, due to dimensions involved much larger than atomic, for energy analysis on the folded graphene structure, and construct a comprehensive map of the size-dependent folding. Here we combine atomistic computations with a continuum model to evaluate the feasibility of folding a graphene sheet. Our result shows that a single fold is not favorable when the size is below 67 Å, and only when the size is more than 210 Å is the double fold more favorable. Overall, it puts the length scale of the smallest origamis into $L \gtrsim 25\text{--}30$ nm.

Results and discussion

Our origami-like elementary structures are made from a square-shaped graphene sheet, as shown in **Figure 1a**. We define the edge in the AC-direction to be along the x -axis, and that in the ZZ-direction to be along the y -axis. Note that x, y can be along any orthogonal directions, because from a linear elasticity standpoint, graphene is an isotropic material.¹⁴ The edge

along y has a length of $L = 5na$, and that along the x -direction is set to be $3\sqrt{3}na$, which is equal to $3\sqrt{3}/5 L \approx 1.04 L$. Here n is the number of repeated units along the x - or y -direction, and $a = 2.42$ Å is the lattice constant of graphene.

By folding this graphene sheet in half along the middle line in the y -direction (the so-called valley fold), and then further folding it at the middle along the x -direction (**Figure 1a**), we obtain the double-folded origami structure. It is a key element (**Figure 1b**) in more complex origami. It represents the simplest possible order-4 vertex,¹⁵ where three valley folds meet with a single mountain fold (in accordance with Maekawa’s theorem for flat-foldable origami^{16,17}).

The double-folded origami consists of four layers, with four edges that have highly different morphologies and terminations. Two adjacent edges are free, and the other two are folded. The optimized (relaxed to minimal energy) geometry of double-folded graphene origami is shown in **Figure 1b**. Notably, the two free edges are not straight, as expected. One of the edges has the two inner layers protrude outward with respect to the two outer (top and bottom) layers. An analogous but weaker effect occurs for the other free edge, where the two middle layers appear to be pulled slightly inward in vicinity of the free AC|ZZ free corner. This is due to the asymmetry of the edges, especially the presence of a double-folded edge and two single-folded edges. As for the two folded edges, one can be created from a folded bilayer origami (**Figure 1b**, bottom), yet the bending along this edge is coupled with a minor structural buckling attributed to the compressive strain in the inner graphene layer; the other is two folded single-layer graphene sheets stacked together (**Figure 1b**, right).

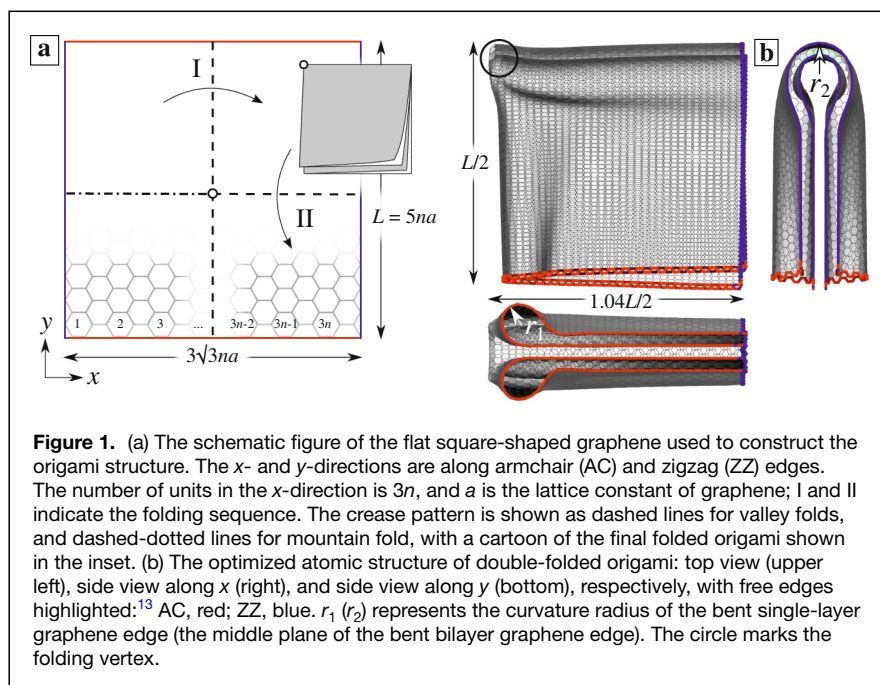
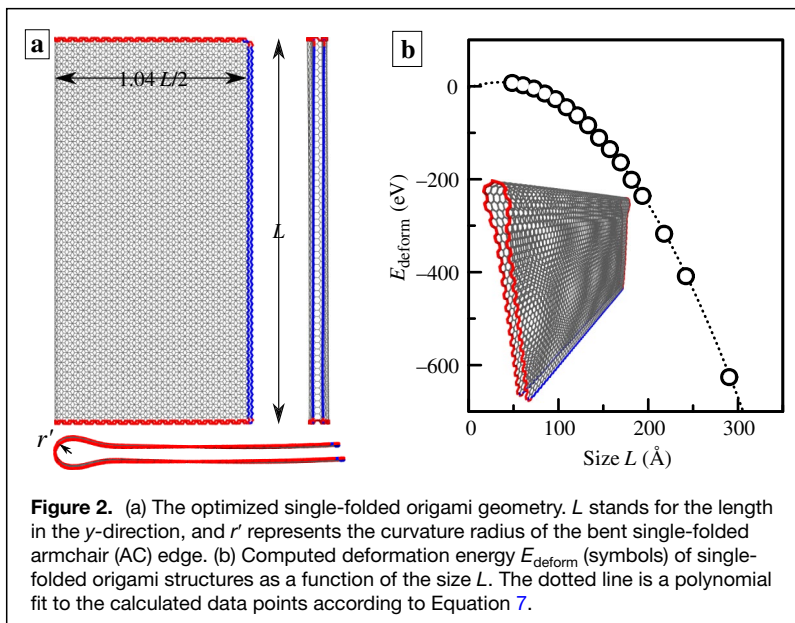


Figure 1. (a) The schematic figure of the flat square-shaped graphene used to construct the origami structure. The x - and y -directions are along armchair (AC) and zigzag (ZZ) edges. The number of units in the x -direction is $3n$, and a is the lattice constant of graphene; I and II indicate the folding sequence. The crease pattern is shown as dashed lines for valley folds, and dashed-dotted lines for mountain fold, with a cartoon of the final folded origami shown in the inset. (b) The optimized atomic structure of double-folded origami: top view (upper left), side view along x (right), and side view along y (bottom), respectively, with free edges highlighted:¹³ AC, red; ZZ, blue. r_1 (r_2) represents the curvature radius of the bent single-layer graphene edge (the middle plane of the bent bilayer graphene edge). The circle marks the folding vertex.



The single-folded origami structures are created using the same set of graphene sheets. By valley-folding the graphene sheet in half along the middle line in the y -direction, we obtain the single-folded origami. This hairpin-like bilayer structure has three free edges, and the other edge is folded; a representative optimized geometry is shown in **Figure 2a**. Details of the computational setup are given in the Methods section.

The deformation energy of double-folded origami has three contributions. One is the bending energy from the two folded edges, which manifests as two folded single-layer graphene sheets stacked together, and one folded bilayer graphene sheet, respectively. The bending energy should be proportional to L . Another term is the energy gain due to vdW attraction between layers, which is proportional to the stacked surface area, thus scaling as $-L^2$. The third one is the energy cost of forming the origami vertex (the circled corner in **Figure 1b**), which should be a constant. Adding up these contributions, the deformation energy can be tentatively written as a quadratic function of L :

$$E_{\text{deform}} = aL^2 + bL + c. \quad (1)$$

The deformation energies calculated as the total energies of an origami geometry relative to that of the respective flat square graphene patch are shown as data points in **Figure 3** and indeed display an inverted parabolic dependence on L . The second-order polynomial in Equation 1 provides an excellent fit, resulting in $a = -0.0157 \text{ eV}/\text{\AA}^2$, $b = 1.88 \text{ eV}/\text{\AA}$, and $c = 7.9 \text{ eV}$. In the formal limit $L \rightarrow 0$, Equation 1 should give the energy cost of the origami vertex (or corner) c_c together with energy (negative) at the triple tip-contacts, evaluated below c' (i.e., together is $c = c_c + 3c' = 7.9 \text{ eV}$). Note that $c \gg k_B T$ but is roughly equivalent in magnitude to the energy of just a single covalent carbon-carbon triple bond and seems to be optimistic, not too prohibitive, for fabricating double-folded origami structures.

We further analyze E_{deform} by breaking it into more specific contributions, not only by different scaling in Equation 1. Analytically, the deformation energy of a double-folded graphene origami can be written as

$$E_{\text{deform}} = E_{\text{bend1}} + E_{\text{bend2}} + E_{\text{vdW}} + E_0, \quad (2)$$

where E_{bend1} is the bending energy of the two stacked folded single-layer graphene, E_{bend2} is the bending energy corresponding to the folded bilayer graphene edge, E_{vdW} is the overall interfacial energy due to vdW interaction between layers (total 4, that is 3 vdW interfaces), and E_0 is the energy of the folding corner. E_{bend1} can be expressed as

$$E_{\text{bend1}} = 1/2 k_b r_1^{-2} S, \quad (3)$$

where k_b is the bending stiffness of graphene that can be determined by calculating the bending energy in straight carbon nanotubes (CNTs), see the Methods section. The bending energy

of a CNT as a function of r^{-2} is plotted in the inset of **Figure 3**. By fitting the LAMMPS results, we obtain $k_b = 0.95 \text{ eV}$ for both zigzag and armchair CNTs, very close to previous empirical-potential values ranging from 0.83 eV to 1.17 eV.^{18,19} S is the equivalent area of the bending section at the edge. Specifically, we take this area as two 3/4 cylinder surfaces with a curvature radius of $r_1 \approx 5 \text{ \AA}$ and a length of $L/2$ (**Figure 1b**). Thus, S can be expressed as $S \approx 3/4 \cdot 2\pi r_1 L$. Similarly, E_{bend2} can be expressed as

$$E_{\text{bend2}} = 1/2 k'_b r_2^{-2} S', \quad (4)$$

where k'_b is the bending stiffness of the folded bilayer graphene, whose value cannot be written immediately but can be obtained later by comparing it with the fitting, and S' is the area of 3/4 cylinder surface. Here we take the curvature radius $r_2 \approx 8.5 \text{ \AA}$ as the value in the middle plane of the bent bilayer graphene, and the length of S' is equal to $1.04L/2$ (**Figure 1b**). Thus $S' \approx 3/4 \cdot 2\pi r_2 \cdot \frac{1.04}{2} L$. On the other hand, there are stacked four layers of square graphene of size $\frac{L}{2} \times 1.04L/2$. Edge corrections need to be considered due to the aforementioned protrusion of the two inner layers with respect to the two outer layers. The area of the protruded bilayer is in the shape of an acute isosceles triangle with an apex angle of $\approx 5^\circ$. Therefore, the overall interfacial energy can be expressed as

$$E_{\text{vdW}} = \left[3 \frac{L}{2} \frac{1.04L}{2} + 2 \left(\frac{1.04L}{2} \right)^2 \sin 5^\circ \right] \gamma, \quad (5)$$

where γ is interfacial energy per unit area, which is $-18.7 \text{ meV}/\text{\AA}^2$ by our calculation. By inserting Equations 3–5 into Equation 2, we analytically obtain the deformation energy of the double-folded origami structure as

$$E_{\text{deform}}^a = -0.0154L^2 + (0.448 + 0.144k'_b)L + E_0. \quad (6)$$

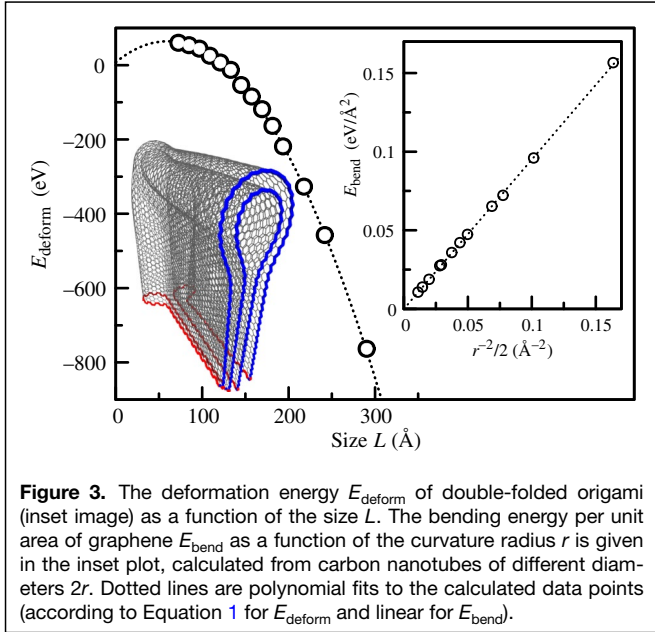


Figure 3. The deformation energy E_{deform} of double-folded origami (inset image) as a function of the size L . The bending energy per unit area of graphene E_{bend} as a function of the curvature radius r is given in the inset plot, calculated from carbon nanotubes of different diameters $2r$. Dotted lines are polynomial fits to the calculated data points (according to Equation 1 for E_{deform} and linear for E_{bend}).

The coefficient of the quadratic term (-0.0154) agrees very well with the direct fitting result above ($a = -0.0157$), supporting the validity of the aforementioned fitting. If we assume the same coefficient of the linear term and the constant term (i.e., $0.448 + 0.144 k'_b = 1.88 \text{ eV/Å}$), we would even obtain $k'_b = 9.94 \text{ eV}$ specifically for the bilayer, and again $E_0 = 7.9 \text{ eV}$. The calculated k'_b is about 10 times higher than k_b . It is reasonable because k'_b is supposed to be larger than k_b due to the increased thickness, but smaller than the no-slip bending stiffness of bilayer graphene (exceeding k_b by ~ 100 times²⁰), since in our case of origami folding, the two layers can slip relative to each other.

Besides the double-folded origami element, we have also evaluated the energetics of single-fold structures, for comparison purposes. Similarly, the energy cost comes from the bending energy of the folded edge, the energy gain originating from the vdW interaction between the two layers, and possibly non-scalable (with L) contribution from the still interacting corner-tips of graphene, c' . The deformation energy of single-folded origami can be written as

$$E_{\text{deform}} = a'L^2 + b'L + 2c'. \quad (7)$$

Calculated results for the left-hand side of Equation 7 are shown in Figure 2b and display a parabolic dependence on L . Fitting using the quadratic function as the right-hand side of Equation 7 gives $a' = -0.0097 \text{ eV/Å}^2$, $b' = 0.69 \text{ eV/Å}$, and $2c' = -3.5 \text{ eV}$. The latter negative value of intercept implies that the edge corner-tips of graphene attract each other, causing some reduction in energy relative to its planar form.

To verify the numerical results, we perform further analysis of E'_{deform} . The deformation energy of a single-folded graphene origami can be analytically expressed as

$$E'^{\text{deform}} = E'_{\text{bend}} + E'_{\text{vdW}} + E'_0, \quad (8)$$

where E'_{bend} is the bending energy of the folded single-layer graphene, E'_{vdW} is the overall interfacial energy due to vdW interaction between layers, and E'_0 is the energy result from the coupling of bending to the edge stress. E'_{bend} can be expressed as

$$E'_{\text{bend}} = 1/2 k_b r'^{-2} S', \quad (9)$$

where $k_b = 0.95 \text{ eV}$, $r' \approx 3.5 \text{ Å}$, $S' \approx (3/4 \pi 3.5 \text{ Å}) \times L$, and therefore $E'_{\text{bend}} = 0.64 \text{ eV/Å} \times L$. The interfacial energy due to vdW interaction can be written as

$$E'_{\text{vdW}} = \gamma L 1.04L/2, \quad (10)$$

hence, the deformation energy can be expressed as

$$E'^{\text{deform}} = -0.0097L^2 + 0.64L + E'_0. \quad (11)$$

The coefficient of the quadratic term (-0.0097) and the linear term (0.64) agrees perfectly with the fitting result ($a' = -0.0097 \text{ eV/Å}^2$, $b' = 0.69 \text{ eV/Å}$). Apparently, $E'_0 = -3.5 \text{ eV}$. With negative energy associated with the two corner-tip contacts ($2c' = -0.35 \text{ eV}$), we can now recover the energy of the double-fold corner as $c_c = c - 3c' \approx 13 \text{ eV}$.

Combining the energy analysis of single- and double-folded graphene structures together, one is able to construct a "phase" diagram, a morphology preference map, as shown in Figure 4, which describes at which size the L form is energetically preferred: flat-planar, single-folded, or double-folded. The purple and green curves are the fitted deformation energies for single-folded and double-folded origami elements, respectively. This diagram reveals a strong size dependence of graphene folding feasibility. We find that all the graphene origamis with different folding multiplicity are energetically stable only when the size of the graphene sheet is larger than

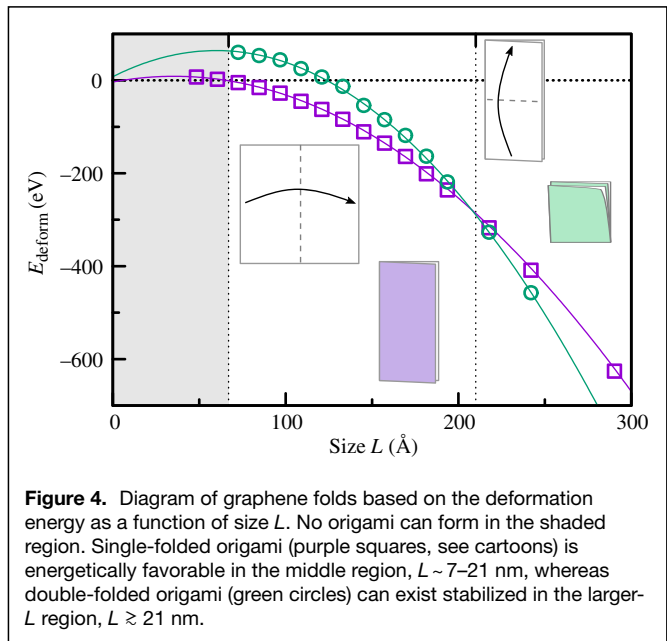


Figure 4. Diagram of graphene folds based on the deformation energy as a function of size L . No origami can form in the shaded region. Single-folded origami (purple squares, see cartoons) is energetically favorable in the middle region, $L \sim 7-21 \text{ nm}$, whereas double-folded origami (green circles) can exist stabilized in the larger- L region, $L \gtrsim 21 \text{ nm}$.



the critical value. When $L > 210 \text{ \AA}$, the double-folded origami structure is the most energetically favorable. While within $67 \text{ \AA} < L < 210 \text{ \AA}$, single-folded, but not higher, origami structures are most stable. For $L < 67 \text{ \AA}$, not even the simplest folded origami structure can form; the graphene energy is dominated by elasticity, and it remains flat. We note that all the numerical results obtained are based on AIREBO potential, which is known to underestimate the stiffness,²¹ k_b . From more realistic density-functional theory (DFT) calculations, it is approximately twice as large (also somewhat varying, depending on the exchange–correlation functionals used). Consequently, the length scale in the map of Figure 4 can be larger, toward $L > 10 \text{ nm}$ for a single fold and $L > 35 \text{ nm}$ for the double fold, an element definitive for any nontrivial origami design.

In the previous analysis, we have only discussed pristine, ideal (single-crystal) graphene at zero temperature (finite temperature and geometry effects on graphene conformation have been studied, for example, in²²). These results can be extended to a more general case considering that the stability of origami increases with the strength of the vdW interaction and decreases with the bending stiffness. Since increasing the temperature reduces the effective interlayer contact area but tends to increase the effective bending stiffness of graphene,²³ the origami becomes overall less stable at a higher temperature. Similarly, polycrystallinity in graphene would disfavor the effective interlayer contact and increase the bending stiffness, thereby lowering the overall stability. It is worth noting that compared to the typical paper origami that are created through irreversible plastic deformation, the graphene origami is entirely different in that they are folded by the ubiquitous vdW adhesion. Therefore, a graphene origami can revert to a perfect graphene sheet upon unfolding.

Conclusion

We found that for nano-origami from graphene, its very name could only be justified to some degree since there is the lower bound, as previously revealed. At too small a length scale, determined by inherent material properties (mostly bending stiffness and surface energy), even the simplest origami element cannot be achieved. We have determined the threshold size for forming single- and double-folded graphene origami elements by large-scale simulations using the AIREBO potential. In particular, the additional energy cost for the folding corner in double-folded origami is estimated to be $\approx 13 \text{ eV}$ (for comparison, this value is nearly twice the energy of a covalent $\text{C}\equiv\text{C}$ triple bond). Since the repeated controlled folding of graphene along arbitrary directions appears to be feasible in practice (e.g., by the tip of a scanning tunneling microscope²⁴), the obtained size-dependent stability domains of graphene origami opens a possibility to guide the formation of origami structures in experiment and invites similar analysis for graphene-derivative-based origami as well.^{25,26}

Methods

All geometry optimization and energy calculations are performed in LAMMPS²⁷ using the AIREBO potential.²⁸ The latter has been shown to accurately capture the bonded interactions between carbon atoms. For the long-range Lennard–Jones term, a cutoff scale factor of 3.0 is used. All structures are fully relaxed using the conjugate gradient method until the force on each atom is less than 10^{-15} eV/\AA . We set the vacuum region to adjacent images in periodic boundary conditions to be over 30 \AA to avoid any spurious interactions. For constructing the origami, we used large graphene square patches, as shown in Figure 1a. To test the influence of the edge termination on the energetics, we have compared graphene sheets with pristine bare edges and hydrogen-terminated edges, finding no quantitative changes in the results. Therefore, we focus on results obtained by using graphene with bare, unpassivated edges. For calculating the bending stiffness, single-walled CNTs with different diameters are routinely used,^{1,19} with periodic images laterally separated by a vacuum region of over 30 \AA . Although the bending stiffness may exhibit some anisotropy in empirical-potential calculations (differing for armchair and zigzag directions),²⁹ the relevant curvatures in this work are deemed too small to cause any nontrivial effect.

Acknowledgments

This work was supported by the US Department of Defense: Air Force Office of Scientific Research (AFOSR), Grant #FA9550-17-1-0262. Z.Z. and Z.H. at NUAA were supported by the Research Fund of State Key Laboratory of Mechanics and Control of Mechanical Structures (No. MCMS-E-0420K01). Computer resources were provided by XSEDE, which is supported by National Science Foundation (NSF) Grant #OCI-1053575, under allocation TG-DMR100029, and the NOTS cluster at Rice University acquired with funds from NSF Grant #CNS-1338099.

References

1. K.N. Kudin, G.E. Scuseria, B.I. Yakobson, C₂F, BN, and C nanoshell elasticity from *Ab Initio* computations. *Phys. Rev. B* **64**(23), 235406 (2001)
2. B.I. Yakobson, C.J. Brabec, J. Bernholc, Nanomechanics of carbon tubes: instabilities beyond linear response. *Phys. Rev. Lett.* **76**(14), 2511 (1996)
3. B.I. Yakobson, R.E. Smalley, Fullerene nanotubes: C_{1,000,000} and beyond. *Am. Sci.* **85**(4), 324 (1997)
4. T. Dumitrica, M. Hua, B.I. Yakobson, Symmetry-, time-, and temperature-dependent strength of carbon nanotubes. *Proc. Natl. Acad. Sci. U.S.A.* **103**(16), 6105 (2006)
5. C. Lee, X. Wei, J.W. Kysar, J. Hone, Measurement of the elastic properties and intrinsic strength of monolayer graphene. *Science* **321**(5887), 385 (2008)
6. F. Liu, P. Ming, J. Li, *Ab Initio* calculation of ideal strength and phonon instability of graphene under tension. *Phys. Rev. B* **76**(6), 064120 (2007)
7. A. Fasolino, J.H. Los, M.I. Katsnelson, Intrinsic ripples in graphene. *Nat. Mater.* **6**(11), 858 (2007)
8. E. Muñoz, A.K. Singh, M.A. Ribas, E.S. Penev, B.I. Yakobson, The ultimate diamond slab: GraphAne versus GraphEne. *Diam. Rel. Mater.* **19**(5–6), 368 (2010)
9. B. Tremi, A. Gillman, P. Buskohl, R. Vaia, Origami mechanologic. *Proc. Natl. Acad. Sci. U.S.A.* **115**(27), 6916 (2018)
10. A.L. Vázquez de Parga, F. Calleja, B. Borca, M.C.G. Passeggi, J.J. Hinarejos, F. Guinea, R. Miranda, Periodically rippled graphene: growth and spatially resolved electronic structure. *Phys. Rev. Lett.* **100**(5), 056807 (2008)



11. M.K. Blees, A.W. Barnard, P.A. Rose, S.P. Roberts, K.L. McGill, P.Y. Huang, A.R. Ruyack, J.W. Kevek, B. Kobrin, D.A. Muller, P.L. McEuen, Graphene Kirigami. *Nature* **524**(7564), 204 (2015)
12. J.Y. Huang, F. Ding, B.I. Yakobson, P. Lu, L. Qi, J. Li, In situ observation of graphene sublimation and multi-layer edge reconstructions. *Proc. Natl. Acad. Sci. U.S.A.* **106**(25), 10103 (2009)
13. A.K. Singh, E.S. Penev, B.I. Yakobson, Armchair or zigzag? A tool for characterizing graphene edge. *Comput. Phys. Comm.* **182**, 804 (2011)
14. L.D. Landau, E.M. Lifshitz, *Theory of Elasticity*, 3rd ed.; Course of theoretical physics (Elsevier: Amsterdam, 1986, vol. 7).
15. S. Waitukaitis, R. Menaut, B.G. Chen, M. van Hecke, Origami multistability: from single vertices to metasheets. *Phys. Rev. Lett.* **114**(5), 055503 (2015)
16. T. Hull, On the mathematics of flat origami. *Congressus Numerantium* **100**, 215 (1994)
17. M. Bern, B. Hayes, The Complexity of Flat Origami, *Proceedings of the Seventh Annual ACM-SIAM Symposium on Discrete Algorithms, SODA* **96**, 175 (1996).
18. M. Arroyo, T. Belytschko, Finite crystal elasticity of carbon nanotubes based on the exponential Cauchy-Born Rule. *Phys. Rev. B* **69**(11), 115415 (2004)
19. J. Tersoff, Energies of fullerenes. *Phys. Rev. B* **46**(23), 15546 (1992)
20. Z. Tu, Z. Ou-Yang, Single-walled and multiwalled carbon nanotubes viewed as elastic tubes with the effective Young's moduli dependent on layer number. *Phys. Rev. B* **65**(23), 233407 (2002)
21. I.V. Lebedeva, A.S. Minkin, A.M. Popov, A.A. Knizhnik, Elastic constants of graphene: comparison of empirical potentials and DFT calculations. *Physica E* **108**, 326 (2019)
22. Z. Xu, M.J. Buehler, Geometry controls conformation of graphene sheets: membranes, ribbons, and scrolls. *ACS Nano* **4**(7), 3869 (2010)
23. B. Sajadi, S. van Hemert, B. Arash, P. Belardinelli, P.G. Steeneken, F. Alijani, Size- and temperature-dependent bending rigidity of graphene using modal analysis. *Carbon* **139**, 334 (2018)
24. H. Chen, X.-L. Zhang, Y.-Y. Zhang, D. Wang, D.-L. Bao, Y. Que, W. Xiao, S. Du, M. Ouyang, S.T. Pantelides, H.-J. Gao, Atomically precise, custom-design origami graphene nanostructures. *Science* **365**(6457), 1036 (2019)
25. O.-K. Park, C.S. Tiwary, Y. Yang, S. Bhowmick, S. Vinod, Q. Zhang, V.L. Colvin, S.A. Syed Asif, R. Vajtai, E.S. Penev, B.I. Yakobson, P.M. Ajayan, Magnetic field controlled graphene oxide-based origami with enhanced surface area and mechanical properties. *Nanoscale* **9** (21), 6991 (2017).
26. Y. Wang, S. Wang, P. Li, S. Rajendran, Z. Xu, S. Liu, F. Guo, Y. He, Z. Li, Z. Xu, C. Gao, Conformational phase map of two-dimensional macromolecular graphene oxide in solution. *Matter* **3**(1), 230 (2020)
27. S. Plimpton, Fast parallel algorithms for short-range molecular dynamics. *J. Comput. Phys.* **117**(1), 1 (1995)
28. S.J. Stuart, A.B. Tutein, J.A.A. Harrison, A reactive potential for hydrocarbons with intermolecular interactions. *J. Chem. Phys.* **112**(14), 6472 (2000)
29. Q. Lu, M. Arroyo, R. Huang, Elastic bending modulus of monolayer graphene. *J. Phys. D* **42**(10), 102002 (2009) □